An Improved Cluster Pair Correlation Method for Obtaining the Absolute Proton Hydration Energy and Enthalpy Evaluated with an Expanded Data Set

William A. Donald and Evan R. Williams*

Department of Chemistry, University of California, Berkeley, California 94720-1460, United States

Received: July 23, 2010; Revised Manuscript Received: September 3, 2010

An improved cluster pair correlation method that is based on the method originally introduced by Tuttle et al. (Tuttle et al. *J. Phys. Chem. A* **2002**, *106*, 925−932) was developed and evaluated using a significantly larger data set than used previously. With this larger data set, values for the absolute proton hydration free energy of −259.3 and −265.0 kcal/mol were obtained using the original and improved method, respectively. The former value is ∼4.5 kcal/mol less negative than previously reported values obtained with the same method but with smaller data sets. The dependence of this value on data set size indicates that the uncertainty in the original method may be greater than previously realized. The improved method has the advantages of higher precision, and the effects of cluster size on the proton hydration free energy and enthalpy values can be more readily evaluated. Data for ions with extreme pK_as, many of which were included in previous estimates of the proton hydration free energy, were found to be unreliable and were eliminated from the extended data set. There is only a subtle effect of cluster size on the Gibbs free energy values, and within the limits of the approximation inherent in the cluster pair correlation method, the "best" value for the standard absolute proton hydration free energy obtained with this new method and larger data set is −263.4 kcal/mol (average for clusters with 4−6 water molecules). The absolute proton hydration enthalpy values decrease from −273.1 to −275.3 kcal/mol with increasing cluster size (one to six water molecules, respectively). This trend, along with an anomalously high value for the absolute proton hydration entropy, indicates that the enthalpy obtained with this method may not have converged for these relatively small clusters.

Introduction

The thermodynamics (ΔG, ΔH, and ΔS) of ion solvation provide valuable information about the band structure of liquid water or other solvents,[1] and the equilibria and dynamics of solution-phase chemical transformations involving charge transfer or neutralization,[2,3] such as for the photosynthetic production of chemical energy or the conversion of stored chemical energy into electrical energy by batteries. Since at least 1920, when Max Born introduced his famous ion solvation equation,[4] there has been much effort devoted to improving and/or developing ever more accurate ion solvation models.[2,3,5−7] More recent state-of-the-art solvation models, such as solvation model 8 (SM8),[6] are useful for computationally investigating the equilibria, dynamics and/or mechanisms of a host of solution-phase charge-transfer processes,[2,3] including those involving free radicals[8] or the redox properties of Fe−S proteins.[9] One of the best ways to evaluate a given solvation model is to compare the calculated solvation energies of various solutes to experimental data.[7,10] However, absolute ion solvation free energies or enthalpies, that is, the energy or enthalpy of transferring an ion at rest in isolation into the bulk of solution at infinite dilution, are not measured directly. The corresponding relative values, that is, the partial thermodynamic contribution of a single ion relative to another ion, can be accurately obtained from solution-phase calorimetric and/or electrochemical measurements.[5,7,10−13] Relative, or conventional, ion solvation energies or enthalpies are commonly referenced to a single ion, the proton, and the relative proton solvation energy or enthalpy (or solvated proton formation energy or enthalpy) is assigned an arbitrary value of exactly 0. Thus, if the absolute solvation energy or enthalpy of a single ion can be determined, the entire relative ion solvation scale can be converted to an absolute ion solvation scale.

As a result of the importance of the absolute thermodynamic values for proton solvation, there has been intense interest in, and efforts toward, obtaining these values from a number of different approaches, including electrochemical measurements,[14−18] direct computations,[19−22] and cluster-based methods.[1,10,11,23−30] Voltaic cell measurements have been used to obtain the "real" proton hydration free energy, which is equal to the sum of the absolute proton hydration energy and the surface potential of bulk water, resulting from the orientation of water molecules at the vapor−water interface.[14−18] Farrell and McTigue reported a value of −260.0 kcal/mol for the real proton hydration free energy that was obtained by extrapolating high-resistance voltaic cell electrochemical measurements to infinite dilution using an electrostatic model,[14] and this value was recommended to the IUPAC by Trasatti in 1986.[15] Because the surface potential of water is not accurately known, comparing absolute ion hydration energies to the real ion hydration energies is challenging, although the potential is believed to be small.[31−34] Depending on how it is defined, the potential of the absolute standard hydrogen electrode (SHE) can be obtained from the atomization free energy of H_2, the ionization free energy of H, a thermodynamic cycle, and *either* the absolute proton hydration free energy *or* the real proton hydration energy.[15,16,35] Using a value for the absolute hydration free energy of the proton is favored by computational chemists,[10,26,35] because it is directly relevant to the ion solvation free energies that are calculated using various ion solvation models, and calculated absolute solution-phase redox potentials can be converted to relative redox values for

* To whom correspondence should be addressed. E-mail: Williams@cchem.berkeley.edu. Phone: (510) 643-7161. Fax: (510) 642-7714.

10.1021/jp1068945
Published on Web 09/23/2010

comparison to experimental redox data. Using the absolute proton hydration free energy to obtain the absolute SHE potential also has the advantage that the potential of the reaction obtained from this reference state depends only on the chemical potentials of the reactants and products and not on the surface potential of water. Values for the absolute proton hydration free energy have been obtained from numerous computations[19−22] by explicitly treating the proton and some number of water molecules in the first or second hydration shell with electronic structure calculations and treating the rest of the bulk solvent with a continuum solvation model.

We have recently developed a new ion nanocalorimetry method,[28−30,36−43] in which the recombination energies of extensively hydrated metal ions upon electron capture in the gas-phase can be obtained from the number of water molecules lost from the reduced precursor and directly related to absolute potentials in bulk solution. From three largely independent hydrated ion nanocalorimetry methods, values for the absolute SHE potential of +4.05, +4.11, and +4.21 V were obtained that are within 5% of each other.[28−30] This method is affected by the surface potential of the water clusters only for ions that reside at the nanodrop surface, which should not be the case for the ions investigated. Thus, these absolute SHE potentials, which are referenced to an electron at infinite distance, are not affected by the value of surface potential of water, and the corresponding standard absolute proton hydration free energy values are −269.1, −267.7, and −265.4 kcal/mol, respectively. The ion nanocalorimetry method is being calibrated using UV laser photodissociation experiments which should improve the accuracy of these absolute proton hydration free energy values. One of the three methods has the advantage that no modeling is required when combined with the laser calibration, making it the most direct measure of an absolute ion reduction potential that is obtained entirely from experimental data.[28]

Values for the absolute proton hydration free energy and enthalpy can be also be obtained by relating data from gaseous measurements of sequential hydration free energies and enthalpies of relatively small clusters[10,11,23−27] to bulk solution using various methods and thermodynamic cycles. Kebarle demonstrated that the difference in the sum of the sequential hydration enthalpies of oppositely charged ions for clusters with up to 8 water molecules approached the absolute difference in bulk solution with increasing cluster size, which supported a value for the absolute proton hydration enthalpy of ∼−270 kcal/mol, which was previously recommended by Desnoyers and Jolicoeur.[45] Klots obtained values for the absolute proton solvation energy (−262.5 kcal/mol) and enthalpy (−271.2 kcal/mol) from the differences in gaseous clustering data between oppositely charged ions, the relative differences in solution, and a clever manipulation of various thermodynamic cycles.[23] In Klots' analysis,[23] data for clusters with only 4 water molecules were considered, and it was assumed that all ions would have the same sequential water molecule binding free energies and enthalpies for $n > 5$.[24] Coe, Tuttle, and co-workers subsequently improved upon this previous work by introducing the cluster pair based approximation method[11] to obtain values for the standard absolute proton hydration energy and enthalpy of −264.0 and −274.9 kcal/mol, respectively, from gaseous measurements for sequential ion and neutral water cluster hydration (for up to 6 water molecules), and bulk relative ion hydration data. Tuttle et al. introduced a similar cluster-based method called the cluster pair correlation scheme,[25] in which data for neutral water clusters is not required, that resulted in essentially the same values for the proton hydration enthalpy and free energy as the cluster pair approximation method. The cluster pair correlation scheme was also used to obtain solvation energies of ions in ammonia using data for clusters with just one ammonia molecule.[25] Kelly et al.[10] used the cluster pair correlation method with a much more extensive ion data set and obtained essentially the same value for the standard absolute proton hydration energy as Tissandier et al.[11] (−264.0 kcal/mol), and used the method to obtain the solvation energies for the proton in methanol (−261.6 kcal/mol), acetonitrile (−258.3 kcal/mol), and dimethyl sulfoxide (−271.4 kcal/mol)[26] using data for clusters with up to three solvent molecules. A similar value for the hydration energy was obtained using calculated water molecule binding energies for clusters with only a single water molecule.[27]

As a result of these cluster pair based methods and the agreement between the various methods from different ion data sets, the value of −264.0 kcal/mol reported by Tissandier et al. is becoming nearly universally accepted. For example, Camaioni and Schwerdtfeger[46] state that "this benchmark experimental value (Tissandier et al.'s reported value)[11] should not be changed unless/until it is superseded by better measurements." Kelly et al. stated,[10] based upon their evaluation of the cluster pair correlation scheme method with a more extensive ion data set than that used by Tissandier et al., that "... we agree with Camaioni and Schwerdtfeger and suggest using a value of −265.9 kcal/mol (corresponding to a standard state value of −264.0 kcal/mol)[11] for the absolute aqueous solvation free energy of the proton in all future applications."

Because of the importance of the values for the absolute proton solvation free energy and enthalpy, and new experimental methods that can be used to measure these values more directly with large clusters where ions are more fully solvated,[28−30] we were interested in investigating the uncertainty with which values can be obtained using the cluster pair correlation method from the available measured ion solvation data. Here, we evaluate this method using a more extensive ion data set than used previously,[10] and introduce an improved method for analyzing the ion hydration data. The effects of ion identity and cluster size upon the values for the proton hydration free energy and enthalpy obtained from this gaseous cluster based method are investigated.

Results and Discussion

Relative and Absolute Ion Solvation Thermodynamics. The standard absolute solvation thermodynamics ($\Delta X_{solv}°(Z) = \Delta G_{solv}°(Z)$ or $\Delta H_{solv}°(Z)$) for transferring an isolated ion (Z) at infinite distance into the bulk of solution are not measured directly. However, relative solvation thermodynamics, $\Delta X_{rel}°(Z)$, of an ion can be obtained accurately from experiments and these values have been tabulated for a large number of ions in various solvents.[5,7,10,12,26] The absolute and relative ion solvation thermodynamic values are related by[10,23]

$$\Delta X_{rel}°(M^+) = \Delta X_{solv}°(M^+) - \Delta X_{solv}°(H^+) \quad (1)$$

and

$$\Delta X_{rel}°(B^-) = \Delta X_{solv}°(B^-) + \Delta X_{solv}°(H^+) \quad (2)$$

where M^+ and B^- are positively and negatively charged ions, respectively. Equations 1 and 2 satisfy the condition that the sum of the $\Delta X_{rel}°(Z)$ values for a given monovalent cation and

SCHEME 1

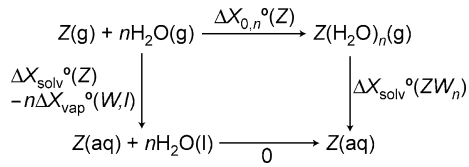

anion pair are equal to the sum of the corresponding absolute values. The values of $\Delta G_{rel}°(Z)$ and $\Delta H_{rel}°(Z)$ for aqueous solution are given in Tables S1 and S2, respectively, in the Supporting Information.[5,7,10−13]

In this work, we report standard hydration energy values for which the standard concentrations are 1 atm of the ion of interest in the gas phase and 1 mol/L in solution, $\Delta G_{solv}°(Z)$ and $\Delta G_{rel}°(Z)$. This is a different reference state than is sometimes reported by others, such as in Kelly et al., where the ion concentrations are 1 mol/L in both the gas and solution phases, indicated by an "*" symbol ($\Delta G_{rel}*(Z)$ and $\Delta G_{solv}*(Z)$).[10] At 298 K, $\Delta G_{rel}*(B^-)$ is 3.8 kcal/mol more negative than $\Delta G_{rel}°(B^-)$, $\Delta G_{rel}*(M^+) = \Delta G_{rel}°(M^+)$, and $\Delta G_{solv}*(Z)$ is 1.9 kcal/mol more negative than $\Delta G_{solv}°(Z)$ values, as discussed by Kelly et al. (page 16067).[10] The relative solvation thermodynamic values used here are referenced to $\Delta X = 0$ for proton solvation, $H^+(g) \rightarrow H^+(aq)$, and not to the heat or free energy for the formation of the hydrated proton. The conversion between these conventions, which differs by the heat of formation of the proton in the gas phase, is described in detail by Kelly et al. (page 16068).[10]

Derivation of the Fundamental Equation of the Cluster Pair Correlation Method. The first step in the derivation of the fundamental equation of the cluster pair correlation method[10,25] is to simply subtract eq 2 from eq 1, and solve for the absolute proton hydration ΔX value, which results in

$$\Delta X_{solv}°(H^+) = (1/2)[\Delta X_{solv}°(M^+) - \Delta X_{solv}°(B^-) - \Delta X_{rel}°(M^+) + \Delta X_{rel}°(B^-)] \quad (3)$$

This equation, which contains three unknown terms, $\Delta X_{solv}°(H^+)$, $\Delta X_{solv}°(M^+)$, and $\Delta X_{solv}°(B^-)$, provides the "scaffold" for the derivation of the cluster pair approximation[11] and the cluster pair correlation[25] methods for obtaining values for the absolute proton solvation energy and enthalpy from gaseous clustering data.

The second step in the derivation involves connecting the absolute hydration ΔX value to the gas-phase sequential hydration ΔX value for a given ion, using the thermodynamic cycle shown in Scheme 1. From this thermocycle, the $\Delta X_{solv}°(Z)$ value is equal to the sum of three terms: (1) the sum of the sequential gaseous ion hydration ΔX values for $Z(H_2O)_n$ from 0 to n water molecules, $\Delta X_{0,n}°(Z)$, (2) the bulk liquid (l) water (W) vaporization ΔX value, $\Delta X_{vap}°(W,l)$, multiplied by n, and (3) the absolute hydration ΔX value of $Z(H_2O)_n$, $\Delta X_{solv}°(ZW_n)$, where W_n is an abbreviation for $(H_2O)_n$; that is

$$\Delta X_{solv}°(Z) = \Delta X_{0,n}°(Z) + n\Delta X_{vap}°(W,l) + \Delta X_{solv}°(ZW_n) \quad (4)$$

The first two terms on the right-hand side of eq 4 can be obtained from experimental measurements. The Gibbs free energies and enthalpies of sequential ion hydration have been measured for many different ions (Tables S3 and S4 of Supporting Information).[47−100] Taking the difference between eq 4 for two oppositely charged monovalent ions results in

$$\Delta X_{solv}°(M^+) - \Delta X_{solv}°(B^-) = \Delta X_{0,n}°(M^+) - \Delta X_{0,n}°(B^-) + \Delta X_{solv}°(MW_n^+) - \Delta X_{solv}°(BW_n^-) \quad (5)$$

The latter two terms of eq 5 go to zero in the limit of infinite n and this equation becomes

$$\Delta X_{solv}°(M^+) - \Delta X_{solv}°(B^-) = \Delta X_{0,\infty}°(M^+) - \Delta X_{0,\infty}°(B^-) \quad (6)$$

Combining eq 6 with eq 3 results in

$$\Delta X_{solv}°(H^+) = (1/2)[\Delta X_{0,\infty}°(M^+) - \Delta X_{0,\infty}°(B^-) - \Delta X_{rel}°(M^+) + \Delta X_{rel}°(B^-)] \quad (7)$$

Gas-phase sequential ion hydration ΔX values can only be measured for finite values of n. Separating $\Delta X_{0,\infty}°(Z)$ into the corresponding terms for 0 to n water molecules and that for $n + 1$ to an infinite number of water molecules in eq 7 results in

$$\Delta X_{solv}°(H^+) = (1/2)[\Delta X_{0,n}°(M^+) - \Delta X_{0,n}°(B^-) + \Delta X°_{n+1,\infty}(M^+) - \Delta X°_{n+1,\infty}(B^-) - \Delta X_{rel}°(M^+) + \Delta X_{rel}°(B^-)] \quad (8)$$

which can be rearranged to the fundamental equation of the cluster pair correlation method[10,25]

$$(1/2)[\Delta X_{0,n}°(M^+) - \Delta X_{0,n}°(B^-)] + (1/2)[\Delta X_{rel}°(B^-) - \Delta X_{rel}°(M^+)] = (1/2)[\Delta X°_{n+1,\infty}(B^-) - \Delta X°_{n+1,\infty}(M^+)] + \Delta X_{solv}°(H^+) \quad (9)$$

where the terms on the left-hand side of the equation can been obtained from experimental data and the terms on the right-hand side are unknown. For the cluster pair correlation scheme, the goal is to find the value of $(1/2)[\Delta X_{rel}°(B^-) - \Delta X_{rel}°(M^+)]$ for a hypothetical ideal cationic and anionic pair, $M^{+\prime}$ and $B^{-\prime}$, such that $\Delta X_{0,n}°(M^{+\prime}) - \Delta X_{0,n}°(B^{-\prime}) = 0$. A key approximation of this method is the implicit assumption that if $(1/2)[\Delta X_{0,n}°(M^{+\prime}) - \Delta X_{0,n}°(B^{-\prime})] = 0$, then $(1/2)[\Delta X_{n+1,\infty}°(B^{-\prime}) - \Delta X_{n+1,\infty}°(M^{+\prime})] = 0$; i.e., if the sequential solvation energies of the hypothetical ideal cation and anion pair are equal at small cluster sizes, these values will also be equal at much larger sizes. To the extent that this assumption is correct, then for the hypothetical ideal ion pair, $(1/2)[\Delta X_{rel}°(B^{-\prime}) - \Delta X_{rel}°(M^{+\prime})] = \Delta X_{solv}°(H^+)$. Tuttle et al.[25] showed that the value of $(1/2)[\Delta X_{rel}°(B^{-\prime}) - \Delta X_{rel}°(M^{+\prime})]$ can be obtained from the intercepts of the best fit lines to plots of $(1/2)[\Delta X_{0,n}°(M^+) - \Delta X_{0,n}°(B^-)] + (1/2)[\Delta X_{rel}°(B^-) - \Delta X_{rel}°(M^+)]$ vs $(1/2)[\Delta X_{rel}°(B^-) - \Delta X_{rel}°(M^+)]$ for many different ion pairs and cluster sizes (for n up to 6). For simplicity, we let

$$\Lambda(M^+, B^-) = (1/2)[\Delta X_{rel}°(B^-) - \Delta X_{rel}°(M^+)] \quad (10)$$

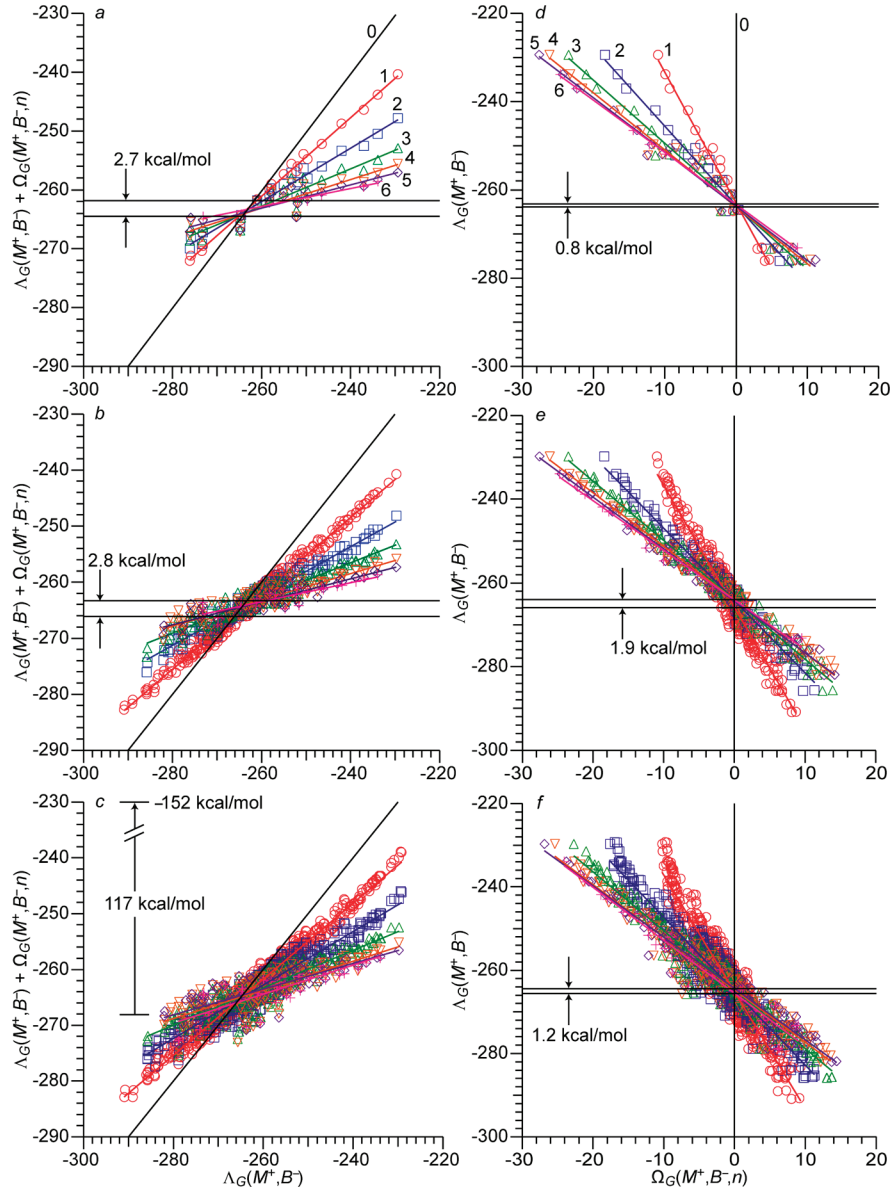

Figure 1. Plots of $\Lambda_G(M^+,B^-) + \Omega_G(M^+,B^-,n)$ vs $\Lambda_G(M^+,B^-)$ using data from (a) Tissandier et al.,[11] (b) Kelly et al.,[10] and (c) the expanded data set, and plots of $\Lambda_G(M^+,B^-)$ vs $\Omega_G(M^+,B^-,n)$ using data from (d) Tissandier et al.,[11] (e) Kelly et al.,[10] and (f) the expanded data set. The ranges in the ordinate values of all the intercept points between each best fit line obtained are indicated by the arrows and the corresponding horizontal lines. Values on both axes in kcal/mol.

and

$$\Omega(M^+, B^-, n) = (1/2)[\Delta X_{0,n}°(M^+) - \Delta X_{0,n}°(B^-)] \quad (11)$$

and note that a plot of $(1/2)[\Delta X_{0,n}°(M^+) - \Delta X_{0,n}°(B^-)] + (1/2)[\Delta X_{rel}°(B^-) - \Delta X_{rel}°(M^+)]$ vs $(1/2)[\Delta X_{rel}°(B^-) - \Delta X_{rel}°(M^+)]$ is equivalent to plotting $\Lambda(M^+,B^-) + \Omega(M^+,B^-,n)$ vs $\Lambda(M^+,B^-)$. Thus, the data on both the *x*- and *y*-axes are significantly dependent upon each other. For Gibbs free energy values, a "G" subscript is used (i.e., $\Lambda_G(M^+,B^-)$ and $\Omega_G(M^+,B^-,n)$) and for enthalpy values an "H" subscript is used (i.e., $\Lambda_H(M^+,B^-)$ and $\Omega_H(M^+,B^-,n)$).

Original Method for Obtaining a Value for $\Delta G_{solv}°(H^+)$ from the Cluster Pair Correlation Method. To evaluate the cluster pair correlation methods, we only include experimental values in our expanded data set that includes data for 55 ions (a total of 1916 data points) and only use the experimental values used by Kelly et al.[10] (36 ions; 787 experimental data points) (see Table S1 of Supporting Information). Kelly et al. also investigated the effects of including an additional 15 ions using calculated $\Delta G_{0,1}(Z)$ values in their analysis, but found that these data did not significantly affect their results.[10] In Figure 1, $\Lambda_G(M^+,B^-) + \Omega_G(M^+,B^-,n)$ values are plotted as a function of $\Lambda_G(M^+,B^-)$ (left panels of Figure 1), for the original data set used by Tuttle et al.[11,25] (Figure 1a), the experimental data set used by Kelly et al.[10] (Figure 1b), and our expanded data set (Figure 1c). A linear regression analysis results in best fit lines for each cluster size (Table 1), with R^2 values that range from 0.773 to 0.996, 0.738 to 0.986, and 0.617 to 0.974 for the Tissandier et al. data set, the Kelly et al. data set, and the expanded data set, respectively. The R^2 values indicate that the plots of $\Lambda_G(M^+,B^-) + \Omega_G(M^+,B^-,n)$ vs $\Lambda_G(M^+,B^-)$ are reasonably linear for the ions used in the analysis, although the scatter in these data increases with data set size. For $n = 0$, $\Omega_G(M^+,B^-,n) = 0$ and the $n = 0$ line is simply $\Lambda_G(M^+,B^-)$ vs $\Lambda_G(M^+,B^-)$ (Figure 1a−c) with a slope of exactly 1. With

TABLE 1: Cluster Pair Correlation Method $y + x$ vs x Best Fit Lines for $n = 1-6$ for Obtaining a Value for $\Delta G_{solv}°(H^+)$[a]

	Tissandier et al.[11] data set			Kelly et al.[10] data set			more extensive data set		
N	*m*	*b*	R^2	*M*	*b*	R^2	*m*	*b*	R^2
0	1	0	1	1	0	1	1	0	1
1	0.67(10)	−87.5(2.5)	0.996	0.677(5)	−86.0(1.2)	0.986	0.68(04)	−84.1(1.07)	0.974
2	0.45(2)	−144.1(4.9)	0.968	0.44(1)	−148.0(2.2)	0.950	0.48(1)	−138.0(1.7)	0.911
3	0.32(3)	−180.2(6.8)	0.889	0.31(1)	−181.4(2.3)	0.891	0.34(1)	−176.0(2.4)	0.803
4	0.24(3)	−200.0(7.0)	0.814	0.23(1)	−202.3(3.1)	0.806	0.26(1)	−196.6(3.9)	0.641
5	0.20(3)	−211.6(6.5)	0.773	0.21(1)	−210.2(3.7)	0.808	0.23(2)	−203.6(5.0)	0.617
6	0.15(1)	−223.5(3.7)	0.937	0.17(2)	−219.8(5.4)	0.738	0.26(3)	−196.9(7.6)	0.674

[a] Slope (*m*) values are unitless and intercept (*b*) values are in kcal/mol.

TABLE 2: Ordinate Values of the Intercepts between Each Best Fit Line from Table 1 for $n = 0-6$ (in kcal/mol) from the $x + y$ vs x Cluster Pair Correlation Method for Obtaining $\Delta G_{solv}°(H^+)$[a]

	n	0	1	2	3	4	5
Tissandier et al. data	1	−263.3(84.7)	–	–	–	–	–
	2	−263.7(18.3)	−263.9(91.0)	–	–	–	–
	3	−264.0(20.2)	−264.3(52.0)	−264.5(69.7)*	–	–	–
	4	−264.1(18.8)	−264.3(38.6)	−264.4(42.3)	−264.3(105.1)	–	–
	5	−263.9(16.5)	−264.0(30.7)	−264.0(31.3)	−263.7(57.9)	−263.2(134.8)	–
	6	−263.3(9.0)	−263.3(18.1)	−263.2(16.4)	−262.9(26.9)	−262.3(43.1)	−261.9(72.7)*
Kelly et al. data	1	−266.1(7.5)*	–	–	–	–	–
	2	−264.4(7.8)	−263.3(16.9)*	–	–	–	–
	3	−264.1(6.9)	−263.5(10.8)	−263.7(27.1)	–	–	–
	4	−264.1(8.0)	−263.8(10.6)	−263.9(18.0)	−264.1(38.1)	–	–
	5	−264.4(9.5)	−264.2(11.8)	−264.4(17.9)	−264.8(30.9)	−266.1(107.0)	–
	6	−264.2(13.3)	−264.0(15.5)	−264.1(20.6)	−264.2(29.3)	−264.3(55.0)	−263.4(93.9)
more extensive data set	1	−265.6(6.8)	–	–	–	–	–
	2	−265.4(6.7)	−265.3(16.7)	–	–	–	–
	3	−265.0(7.2)	−264.8(11.4)	−264.5(23.8)	–	–	–
	4	−265.0(10.6)	−264.8(13.9)	−264.7(20.9)	−264.9(49.5)	–	–
	5	−264.7(13.2)	−264.5(16.4)	−264.3(22.6)	−264.1(42.6)	−262.6(159.7)	–
	6	−266.0(20.8)	−266.1(26.2)	−266.4(37.7)	−268.3(85.6)*	−151.7(2786.6)*	−256.5(198.6)

[a] The upper limit to the uncertainty is indicated in parentheses, which are obtained from propagation of the uncertainty in the slopes and intercepts of the best fit lines. Asterisks indicate the smallest and largest values obtained for each data set. Data sets used to obtain these values are from Tissandier et al.,[11] Kelly et al.,[10] and the expanded data set (Tables S1 and S3).

increasing cluster size, the slopes of the best fit lines decrease because the *y*-axis values, $\Omega_G(M^+,B^-,n) + \Lambda_G(M^+,B^-)$, approach a constant value with increasing cluster size, which at infinite cluster size is equal to the absolute proton hydration free energy for any given ion pair (eq 9). At the points of intersection between any two lines, $\Omega_G(M^+,B^-,n) = 0$, and the $\Lambda_G(M^+,B^-)$ ordinate value at the intersection between these two lines corresponds to $(1/2)[\Delta X_{n+1,\infty}°(B^{-\prime}) - \Delta X_{n+1,\infty}°(M^{+\prime})] + \Delta X_{solv}°(H^+)$. The implicit assumption with this method is that $(1/2)[\Delta X_{n+1,\infty}°(B^{-\prime}) - \Delta X_{n+1,\infty}°(M^{+\prime})] = 0$, and that $\Delta X_{solv}°(H^+)$ can be obtained directly from the intercepts of any two lines. For the 7 lines in these plots (6 best fit lines and the $n = 0$ line) there are 21 points where any 2 of the 7 lines intersect and the ordinate values for each intersection point for all three sets of data are given in Table 2. Tuttle et al.[25] and Kelly et al.[10] calculated the average of the ordinate values for each of the intersection points (21 points in all) to obtain a value for the absolute standard proton hydration free energy of −263.6 and −264.0 kcal/mol, respectively, which are the same values we obtain using the same method and same data. A significantly less negative value of −259.3 kcal/mol is obtained with this method from the larger data set. The ~4.5 kcal/mol less negative value obtained when more data are included indicates that the uncertainty in the previously reported absolute proton hydration free energy value obtained from the cluster pair correlation method may be much larger than previously appreciated.

Tuttle et al.[25] noted that, when the slopes of any two lines are similar, the value of the intersection point can be far from the average of all the intercept values; that is, the uncertainty in the intersection points is greatest for lines that have similar slopes. In Table 2, we list the ordinate intersection points and the upper limit to the uncertainty in these values obtained by propagating the uncertainty in the slope and intercept of the best fit lines (see Supporting Information). Because the uncertainties in the slope and intercept of any line are strongly correlated, these propagated uncertainty values represent gross upper limits to the actual uncertainty. Although these are upper limits, they can be used to compare the extent of uncertainty for each intersection point relative to the uncertainty propagated for the other intercept values. Values with the least uncertainty are generally obtained from intersection points between any of the $n = 1-6$ best fit lines and the $n = 0$ line (Table 2). An extreme example of the uncertainty introduced when the intersection point of two lines with similar slopes are used is the intersection point between the $n = 4$ and $n = 6$ best fit lines for the expanded data set (Figure 1c). Because the slopes of the $n = 4$ and 6 best fit lines are nearly the same, i.e., nearly parallel, the ordinate value at the intersection point is −151.7 kcal/mol, which is 107.6 kcal/mol higher than the average of all the intersection points! More accurate values could be obtained by only considering the intersection points of each best fit line with the $n = 0$ lines. For example, the average and standard deviations of the of the intercept values of the $n = 1-6$ best fit lines with the $n = 0$ line are −265.3 and 0.5 kcal/mol, respectively, compared to the corresponding values of −259.3 and 24.8 kcal/mol obtained from the average of all the data points (most extensive data set).

TABLE 3: Cluster Pair Correlation x vs y Method Best Fit Lines for $n = 1-6$ for Obtaining $\Delta G_{solv}°(H^+)$[a]

	Tissandier et al. data set			Kelly et al. data set			more extensive data set		
N	m	b	R^2	M	b	R^2	m	b	R^2
1	−2.96(9)	−263.2(4)	0.985	−2.91(4)	−265.9(2)	0.941	−2.81(4)	−265.2(1)	0.889
2	−1.79(6)	−263.5(5)	0.978	−1.73(3)	−264.3(2)	0.968	−1.78(2)	−265.1(1)	0.923
3	−1.43(6)	−263.8(6)	0.974	−1.42(2)	−264.0(2)	0.975	−1.42(2)	−264.7(2)	0.941
4	−1.29(5)	−263.9(6)	0.977	−1.28(2)	−264.0(2)	0.978	−1.26(3)	−264.7(2)	0.936
5	−1.23(4)	−263.7(5)	0.982	−1.24(2)	−264.3(3)	0.984	−1.23(3)	−264.4(3)	0.947
6	−1.18(2)	−263.3(3)	0.998	−1.18(3)	−264.1(4)	0.986	−1.28(5)	−265.6(5)	0.944

[a] Slope (m) values are unitless and intercept (b) values are in kcal/mol.

TABLE 4: Values for $\Delta G_{solv}°(H^+) + (1/2)[\Delta G_{n+1,\infty}(B^{-\prime}) - \Delta G_{n+1,\infty}(M^{+\prime})]$ (in kcal/mol) Obtained Using the $x + y$ vs x Cluster Pair Correlation Method and the Improved x vs y Method

	Tissandier et al. data			Kelly et al. data			more extensive data set		
	$x + y$ vs x		x vs y	$x + y$ vs x		x vs y	$x + y$ vs x		x vs y
n	$\langle Y_0\rangle$[a]	$SD_{\langle Y\rangle}$	b[c]	$\langle Y_0\rangle$[a]	$SD_{\langle Y\rangle}$	b[c]	$\langle Y_0\rangle$[a]	$SD_{\langle Y\rangle}$	b[c]
0	−263.7(27.9)	0.4	−	−264.5(8.8)	0.8	−	−265.3(10.9)	0.5	−
1	−263.8(52.5)	0.4	−263.2(4)	−264.1(12.2)	1.0	−265.9(2)	−265.2(15.2)	0.6	−265.2(1)
2	−264.0(44.9)	0.5	−263.5(5)	−264.0(18.1)	0.4	−264.3(2)	−265.1(21.4)	0.8	−265.1(1)
3	−264.0(55.3)	0.6	−263.8(6)	−264.1(23.8)	0.4	−264.0(2)	−265.3(36.7)	1.5	−264.7(2)
4	−263.8(63.8)	0.8	−263.9(6)	−264.4(39.4)	0.9	−264.0(2)	−245.6(506.9)	46.0	−264.7(2)
5	−263.4(57.3)	0.8	−263.7(5)	−264.5(45.2)	0.9	−264.3(3)	−262.8(75.5)	3.1	−264.4(3)
6	−262.8(31.0)	0.6	−263.3(3)	−264.0(37.9)	0.3	−264.1(4)	−245.8(525.9)	46.3	−265.6(5)
all	−263.6(47.5)[b]	0.7	−263.6(5)[d]	−264.2(26.5)[b]	0.7	−264.4(2)[d]	−259.3(170.4)[b]	24.8	−265.0(2)[d]

[a] Obtained from the intercept of each best fit line for the indicated cluster size with the other 6 lines. For $x + y$ vs x method, the propagated uncertainty is given in parentheses and is an upper limit to the uncertainty in the corresponding intercept value. Standard deviation values (SD) are lower limits to the uncertainty. [b] Obtained from the average of all 21 intercepts of the best fit lines. [c] Obtained from the y-axis intercepts (b) of the best fit lines to the x vs y plots. [d] The average of the intercept values of the best fit lines for each cluster size ($n = 1-6$).

Improved Method for Obtaining a Value for $\Delta G_{solv}°(H^+)$ from the Cluster Pair Correlation Method. To compensate for the fact that the ordinate value of the intersection points between best fit lines with similar slopes have more uncertainty than that for lines that have a greater difference between the slopes, Tuttle et al.[25] reported the average of all the ordinate intercept points weighted by a fraction relating the difference in the slope of the two intersecting lines to the sum total of the difference in slope between all the other lines. Rather than weight the ordinate values obtained from the intersection points of each line, we found that the uncertainty in the $(1/2)[\Delta G_{n+1,\infty}°(B^{-\prime}) - \Delta G_{n+1,\infty}°(M^{+\prime})] + \Delta G_{solv}°(H^+)$ values obtained from the cluster pair correlation scheme can be dramatically reduced by simply plotting $\Lambda_G(M^+,B^-)$ vs $\Omega_G(M^+,B^-,n)$, fitting the data with a linear regression analysis, and obtaining the y-axis intercept of these best fit lines for each n (Figure 1d−f; see Table 3 for parameters of best fit lines). Thus, the data plotted on the x- and y-axes are significantly less correlated than for the traditional method of plotting $\Lambda_G(M^+,B^-) + \Omega_G(M^+,B^-,n)$ vs $\Lambda_G(M^+,B^-)$. When plotted this new way, the y-axis intercept is the value of $\Lambda_G(M^+,B^-)$ for which $\Omega_G(M^+,B^-,n) = 0$, which corresponds to the value of $\Delta G_{solv}°(H^+) + (1/2)[\Delta G_{n+1,\infty}°(B^{-\prime}) - \Delta G_{n+1,\infty}°(M^{+\prime})]$ (see eq 9). From here on, we refer to this as the x vs y method of plotting the data, as opposed to the $y + x$ vs x method that was previously[10,25] used. This x vs y method of plotting the data has the advantage that both the range and uncertainty in the values obtained for $\Delta G_{solv}°(H^+) + (1/2)[\Delta G_{n+1,\infty}°(B^{-\prime}) - \Delta G_{n+1,\infty}°(M^{+\prime})]$ are significantly reduced (Table 4), especially for cases where the $y + x$ vs x method results in lines that are nearly parallel (see Figure 1, c vs f). For example, for the most extensive data set, the $y + x$ vs x method of plotting the data results in 21 intersection points with an average ordinate value of −259.3 kcal/mol and a standard deviation of 24.8 kcal/mol. By contrast, simply plotting same data as x vs y results in 6 best fit lines with an average y-axis intercept of −265.0 kcal/mol and a standard deviation of only 0.4 kcal/mol. Thus, the absolute proton hydration free energy value obtained using this new method is 5.7 kcal/mol more negative than that obtained with the conventional[25] cluster pair correlation method using the same extended data set.

In addition to providing a much more negative absolute proton hydration free energy value, this method results in significantly better precision. The upper limit of the uncertainty in the intercept values, i.e., the propagated uncertainty, is only 2 kcal/mol for the x vs y method vs 170 kcal/mol for the $y + x$ vs x method. The improved uncertainty is a result of (1) the better linear correlation obtained from plotting x vs y compared to $y + x$ vs x (Table 1 vs Table 3), and (2) the intercept values are generally obtained from intersecting lines with larger angles between the lines for the x vs y plot than for the $y + x$ vs x plots. For example, 17 out of 18 of the best fit lines obtained from the x vs y plots for each of the three data sets have R^2 values greater than 0.9 (Table 3). This is in contrast to the lines obtained from plotting $y + x$ vs x, for which only 7 out of the 18 best fit lines have R^2 values or greater than 0.9, and some have R^2 values as low as 0.6. Also, for the x vs y plots, the angles between the intersecting lines (between the $n = 1-6$ best fit lines and the y-axis) approach 45° with increasing n, whereas for the $y + x$ vs x method these angles can be considerable less (nearly 0° in the case of the $n = 4$ and 6 lines for the most extensive data set). Thus, from here on, we only use the x vs y method of plotting the data to obtain values for $\Delta G_{solv}°(H^+) + (1/2)[\Delta G_{n+1,\infty}°(B^{-\prime}) - \Delta G_{n+1,\infty}°(M^{+\prime})]$.

Effects of Cluster Size and Ion Data Set on $\Delta G_{solv}°(H^+)$. The other advantage of plotting the data as x vs y is that effects of cluster size on the values obtained for $(1/2)[\Delta G_{n+1,\infty}°(B^{-\prime}) - \Delta G_{n+1,\infty}°(M^{+\prime})] + \Delta G_{solv}°(H^+)$ can be more readily investigated because the values are obtained from a line corresponding to a single cluster size intersecting with only the y-axis and not

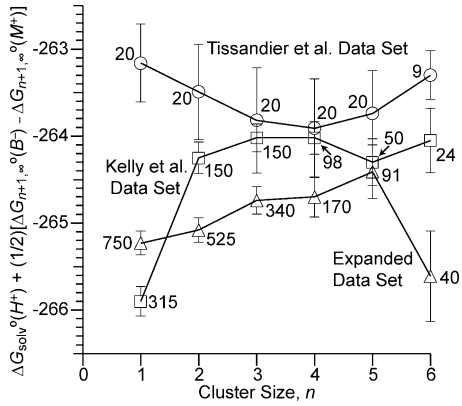

Figure 2. Values of $\Delta G_{solv}°(H^+) + (1/2)[\Delta G_{n+1,\infty}(B^-) - \Delta G_{n+1,\infty}(M^+)]$ (in kcal/mol) obtained from the *y*-axis intercepts of the best fit lines to the $\Lambda_G(M^+,B^-)$ vs $\Omega_G(M^+,B^-,n)$ plots in Figure 1d−f using data from Tissandier et al.[11] (open circles), Kelly et al.[10] (open squares), and the expanded data set (open triangles). The number next to each symbol indicates the number of data points fit to obtain each intercept value.

with any of the other lines that correspond to other cluster sizes; that is, the *x* vs *y* method gives intercept values for each cluster size that are more independent of the other cluster sizes.[101] Furthermore, the intercept values obtained from the *x* vs *y* method generally have less uncertainty, which should make it easier to determine if the differences in the intercept values obtained for different clusters size or ion data sets are significant. Values for $\Delta G_{solv}°(H^+) + (1/2)[\Delta G_{n+1,\infty}°(B^{-\prime}) - \Delta G_{n+1,\infty}°(M^{+\prime})]$ as a function of cluster size (Figure 2) vary between −266 and −263 kcal/mol depending on the data set and on the cluster size used, and there does not appear to be any strong trend with cluster size.

Relative Solvation Energies of Protonated and Deprotonated Ions. Because $\Delta G_{solv}°(H^+)$ is a constant value, differences between the values obtained from the cluster pair correlation method from different ion sets and cluster sizes can be the result of differences in $(1/2)[\Delta G_{n+1,\infty}°(B^{-\prime}) - \Delta G_{n+1,\infty}°(M^{+\prime})]$ values and/or uncertainties in the experimental data itself. Gaseous sequential ion hydration and solution-phase relative ion solvation ΔX values both are used in the cluster pair approximation, and uncertainties in these measurements affect the uncertainty of the values for the proton hydration free energy and enthalpy obtained from the method. Values for sequential ion hydration free energies and enthalpies from equilibrium mass spectrometry and guide ion-beam measurements usually have an uncertainty of around ±1 kcal/mol. By contrast, obtaining accurate relative ion solvation free energies and enthalpies for ions with extreme pK_a values referenced to dilute aqueous solution at neutral pH is very challenging. In this and the next section, we consider effects of large uncertainties in the relative solvation energies for ions with extreme pK_a values.

The relative ion solvation energies of deprotonated neutral molecules, $\Delta G_{rel}°(A^-)$, can be obtained from the gas-phase basicity of the deprotonated ion, $\Delta G_{GB}°(A^-)$, the solvation energy of the neutral molecule, $\Delta G_{solv}°(HA)$, the pK_a of the neutral molecule (corresponding to the Gibbs free energy of solution-phase deprotonation $\Delta G_{pK}°(HA)$), and the Scheme 2 thermodynamic cycle, from which[5,7,10]

$$\Delta G_{rel}°(A^-) = -\Delta G_{GB}°(A^-) + \Delta G_{solv}°(HA) + \Delta G_{pK}°(HA) \quad (12)$$

SCHEME 2

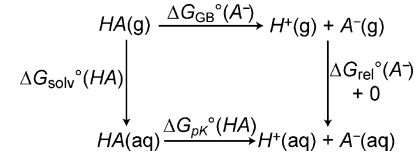

SCHEME 3

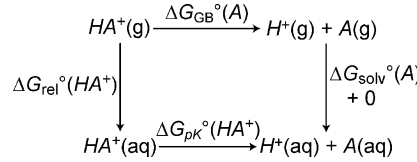

An analogous equation can be obtained for the relative solvation energy of a protonated neutral molecule, $\Delta G_{rel}°(HA^+)$, from the solvation energy of the neutral molecule, $\Delta G_{solv}°(A)$, the gas-phase basicity of the neutral molecule, $\Delta G_{GB}°(A)$, the pK_a of the protonated molecule (corresponding to $\Delta G_{pK}°(HA^+)$), and the Scheme 3 thermodynamic cycle (eq 13):[5,7,10]

$$\Delta G_{rel}°(HA^+) = \Delta G_{GB}°(A) + \Delta G_{solv}°(A) - \Delta G_{pK}°(HA^+) \quad (13)$$

The relative ion solvation energies of an extensive set of protonated and deprotonated neutrals have been previously tabulated[5,7,10] using these thermodynamic cycles and the corresponding Gibbs free energy data obtained from experiment. However, it is important to consider that the pK_a values of extremely strong acids and the pK_a values of the conjugate acids (HA) of extremely strong bases (A^-, referred to here as pK_a of a base) are difficult to measure directly in dilute aqueous solutions at neutral pH because of the intrinsic limits set by the autoprotolysis constant of water.[102−104] For example, the pK_a of acetylene is estimated to be ∼25,[105,106] so there should be only 1 HCC^-(aq) for every 10^{18} HCCH(aq) in neutral water containing acetylene. Thus, accurately measuring extreme pK_a values in dilute aqueous solutions is a highly challenging analytical problem. Instead, extreme pK_a values of extremely strong acids and bases are routinely measured in a variety of nonaqueous solvents and referenced to dilute aqueous solutions using acidity functions that relate the pK_a of a species in a nonaqueous solvent or strongly acidified (or a strongly basic) aqueous solution to the pK_a of the species in dilute aqueous solution at neutral pH.[102−104] As a result, the reported pK_a of various species with extreme pK_a values are generally estimates for these values in dilute aqueous solution.

Effects of Using Extremely Strong Acidic and Basic Ions on the Cluster Pair Correlation Method. Because of potential uncertainties of pK_a values for ions with extreme pK_as in dilute aqueous solution at neutral pH, we investigated the effect of these ions on the cluster pair correlation method. There are 11 ions in the more extensive data set (Table S1) that have pK_a values that are less than 0 or greater than 14 (with the exception of H_3O^+ and OH^-). We use the relative solvation energies for the ions with extreme pK_a values that were compiled by Kelly et al.[5] (acetylene, methanol, 5 oxonium ions, protonated pyrrole, acetonitrile, and dimethyl sulfoxide) and Pliego et al.[7] (protonated acetamide). In Figure 3, $\Lambda_G(M^+,B^-)$ is plotted as a function of $\Omega_G(M^+,B^-,n)$ using data for ions with reported pK_a values between 0 and 14 (and including data for H_3O^+ and OH^-) in addition to protonated acetonitrile, which has the most

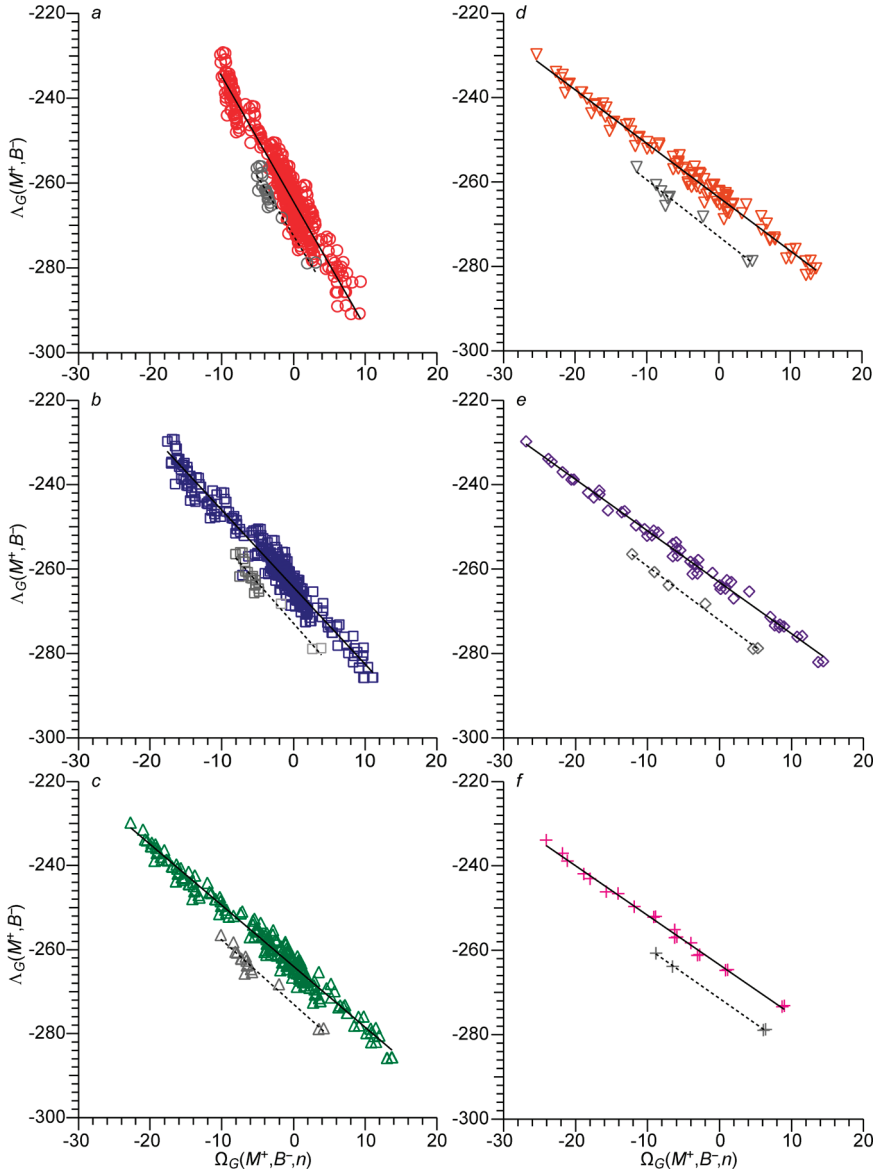

Figure 3. $\Lambda_G(M^+,B^-)$ vs $\Omega_G(M^+,B^-,n)$, for $n = 1-6$ (a−f, respectively), using data for ions that are not extremely strong acids ($pK_a < 0$, except for H_3O^+) and ions that are not extremely basic (pK_a of conjugate acid >14, except for OH^-) (colored symbols). Gray symbols indicate data points that include data for protonated acetonitrile (using a pK_a value of −10). Solid lines are best fit lines of all the data, and dashed gray lines are best fit lines of the only the data points that include data for protonated acetonitrile. Values on both axes in kcal/mol.

extreme pK_a value (∼−10)[107] of any of the ions used in this work. Reported pK_a values for protonated acetonitrile range from ∼−4 to −11,[107−109] although most estimates appear closer to a value of ∼−11.[108] In general, the $\Lambda_G(M^+,B^-)$ values for data points that include protonated acetonitrile data are ∼7 kcal/mol lower than that for the other data points at a given $\Omega_G(M^+,B^-,n)$ value (Figure 3).

The cluster pair correlation method can be tested for a given ion by iteratively solving for the ion pK_a value that minimizes the deviation between the best fit line of all the $\Lambda(M^+,B^-)$ vs $\Omega(M^+,B^-,n)$ data points and the best fit line for the data points that include only the ion of interest. For example, the average absolute deviation of the $\Lambda(M^+,B^-)$ values that include protonated acetonitrile from the best fit line for all of the data points range from ∼6.0 to 8.0 kcal/mol using a pK_a value of −10 for acetonitrile. For each cluster size, the pK_a value of protonated acetonitrile can be optimized such that the average absolute deviation between the $\Lambda(M^+,B^-)$ vs $\Omega(M^+,B^-,n)$ data points for those that include data for protonated acetonitrile and all the other data points is minimized. From this optimization, pK_a values for protonated acetonitrile of between +2.7 and +1.0 for $n = 1$ to 6 are obtained. These values are *dramatically* higher than the previously reported values for this ion (∼−4 to −11).[107−109]

In Figure 4, the optimized pK_a values obtained from the cluster pair correlation method for all of the ions with extreme pK_a values are plotted as a function of the literature pK_a values, for each cluster size. The optimized pK_a values obtained for protonated dimethyl sulfide ($n = 1$ and 2), protonated formamide ($n = 2-5$), and methanol ($n = 2$) are relatively close to the literature value (within 1 pK_a unit).[7,102] However, the optimized pK_a values obtained from the cluster pair correlation method are significantly larger than the estimated values for the other ions. For example, the optimized pK_a value for protonated acetophenone is 3 and 4 (for $n = 1$ and 2, respectively), whereas the value reported in aqueous solution is ∼−4.3![102] These results suggest that data for larger clusters may be required to obtain accurate pK_a values for such ions using the cluster pair correlation method.

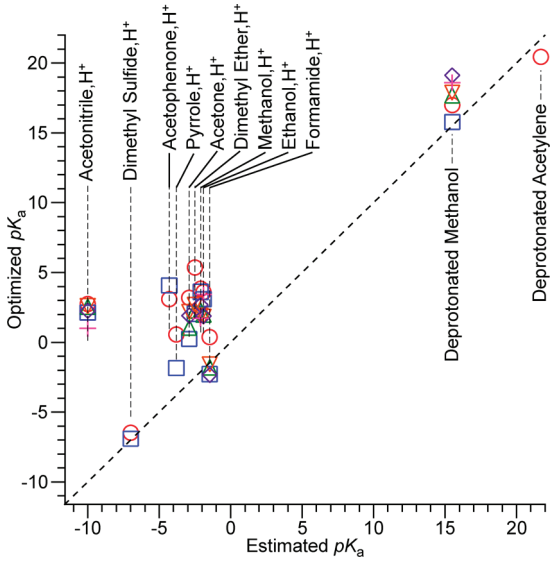

Figure 4. Optimized pK_a values obtained from the cluster pair correlation scheme vs the estimated pK_a values[5,7] for ions that are extremely acidic and extremely basic, for $n = 1$ (○), 2 (□), 3 (△), 4 (▽), 5 (◇), and 6 (+). pK_as for extremely basic ions (B^-) refer to the pK_a of the conjugate acid (BH).

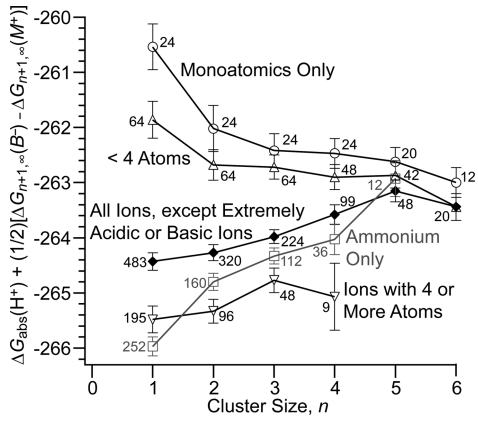

Figure 5. Values of $\Delta G_{solv}°(H^+) + (1/2)[\Delta G_{n+1,\infty}(B^-) - \Delta G_{n+1,\infty}(M^+)]$ (in kcal/mol) obtained from the intercepts of the best fit lines to the $\Lambda_G(M^+,B^-)$ vs $\Omega_G(M^+,B^-,n)$ plots using data for ions with 3 or fewer atoms (and NH_4^+, △), 4 or more atoms (except NH_4^+, ▽), monatomic ions only (○), ammonium ions with all anions (□), and all ions (◆). None of these data sets include the 11 extremely basic or acidic ions listed in Figure 4. The numbers near each symbol indicate the number of data points fit to obtain the corresponding intercept value.

Effect of Ion Identity on Cluster Pair Correlation Method. Because of the difficulty in determining the relative ion solvation energies for ions with extreme pK_a values, we obtained the values of $\Delta G_{solv}°(H^+) + (1/2)[\Delta G_{n+1,\infty}°(B^{-\prime}) - \Delta G_{n+1,\infty}°(M^{+\prime})]$ using the same data set as in Tables S1 and S3 (of Supporting Information), but removed the 11 ions with extreme pK_a values (see the ions listed in Figure 4). A qualitatively similar trend in $\Delta G_{solv}°(H^+) + (1/2)[\Delta G_{n+1,\infty}°(B^{-\prime}) - \Delta G_{n+1,\infty}°(M^{+\prime})]$ values is observed (Figure 5), but these values are on average 1.2 kcal/mol less negative than when the ions with extreme pK_a values are included.

Kelly et al.[10] reported that the absolute proton hydration free energy values obtained from the cluster pair correlation method depend on the number and type of ions used. To investigate this effect with the larger data set, these data were broken into general arbitrary categories. For monotonic ions, or ions including three or fewer ions (and NH_4^+ because of its relatively small physical size), the values generally decrease with increasing cluster size. For the larger ions (four or more atoms, ▽ symbols), the values are significantly lower, and for ammonium cations, the values increase with increasing cluster size. Because the proton solvation free energy value is a constant value, these data indicate that the value of $(1/2)[\Delta G_{n+1,\infty}°(B^{-\prime}) - \Delta G_{n+1,\infty}°(M^{+\prime})]$ depends on both the ion identity and on the cluster sizes used in the analysis. $(1/2)[\Delta G_{n+1,\infty}°(B^{-\prime}) - \Delta G_{n+1,\infty}°(M^{+\prime})]$ should approach 0 with increasing cluster size, so that the most accurate values for $\Delta G_{solv}°(H^+)$ should in principle be obtained from the largest clusters. These results suggest that a more accurate value for $\Delta G_{solv}°(H^+)$ could be obtained from data for larger clusters, although such experimental data is sparse.

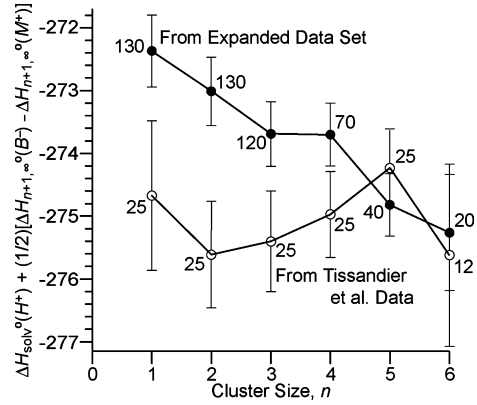

Figure 6. Values of $\Delta H_{solv}°(H^+) + (1/2)[\Delta H_{n+1,\infty}(B^-) - \Delta H_{n+1,\infty}(M^+)]$ (in kcal/mol), obtained from the intercepts of the best fit lines to the $\Lambda_H(M^+,B^-)$ vs $\Omega_H(M^+,B^-,n)$ plots using data from Tissandier et al. (open circles) and from the expanded data set in Tables S2 and S4 (closed circles), as a function of cluster size. The numbers near each symbol indicate the number of data points fit to obtain the corresponding intercept value.

Effects of Cluster Size and Ion Data Set on $\Delta H_{solv}°(H^+)$ Values Obtained from the Cluster Pair Correlation Method. A value for the proton solvation enthalpy can also be obtained from the cluster pair correlation method in an analogous manner. In Figure 6, values of $\Delta H_{solv}°(H^+) + (1/2)[\Delta H_{n+1,\infty}°(B^-) - \Delta H_{n+1,\infty}°(M^+)]$ were obtained from a plot of $\Lambda_H(M^+,B^-)$ vs $\Omega_H(M^+,B^-,n)$ using the enthalpy data set from Tissandier et al. (open circles) that includes data for 9 ions and a more extensive data set for 23 ions (filled circles) that are listed in Tables S2 and S4 (see Supporting Information). Values of $\Delta H_{solv}°(H^+) + (1/2)[\Delta H_{n+1,\infty}°(B^-) - \Delta H_{n+1,\infty}°(M^+)]$ obtained using the Tissandier et al. data are relatively constant as a function of cluster size (between −275.7 and −274.2 kcal/mol). In contrast, values obtained using the more extensive data set decrease from a value of −273.1 kcal/mol for $n = 1$ to a value of −275.3 kcal/mol for $n = 6$, with increasing cluster size. These results indicate that the value of $(1/2)[\Delta H_{n+1,\infty}°(B^-) - \Delta H_{n+1,\infty}°(M^+)]$ also depends on the ion identities and cluster sizes used in the cluster pair correlation method analysis. The stronger dependence on cluster size for the enthalpy values vs the free energy values could be a result of the larger uncertainty that is often associated with enthalpy values, which are obtained from the temperature dependence of free energy values in equilibrium experiments, than for free energy values, which can be obtained from a measurement at a single temperature. Alternatively, convergence to a constant $\Delta X_{solv}°(H^+)$ with increasing cluster size may be different for free energies and enthalpies.

Absolute Proton Hydration Entropy. Although the absolute proton solvation Gibbs free energy and entropy are not directly measured in solution, the absolute proton solvation entropy can

be measured using nonisothermal electrochemical measurements by varying the temperature of one half-cell referenced to another half-cell at a constant temperature.[110−112] From these measurements, the absolute entropy of half-cell reactions and standard single ion entropies in aqueous solution can be determined. Conway and co-workers measured the temperature dependence of the hydrogen electrode (0.878 ± 0.003 mV/K),[110] which is in very good agreement with the earlier value reported by de Bethune.[111] From this data, a value of −30.7 ± 0.7 cal/(mol·K) for the absolute proton solvation entropy is obtained,[113] which is in excellent agreement with the value of −30.8 ± 0.3 cal/(mol·K) obtained from an average of 10 reported values for the standard entropy of the aqueous proton from various experimental methods.[112] The directly measured value for the absolute proton solvation entropy (−30.7 cal/(mol·K)) can be compared to the values obtained from the cluster pair correlation method. A value of −39.8 cal/(mol·K) for the absolute proton solvation entropy is obtained from the difference in the enthalpy value (−275.3 kcal/mol) obtained from the largest cluster size in Figure 6 (for the more extensive data set; closed circles), and Gibbs free energy value of −263.4 kcal/mol obtained from the average of the $n = 4-6$ data points in Figure 5 (for the more extensive data set; closed diamonds). A proton hydration entropy value of −36.6 cal/(mol·K) is obtained from the Tissandier et al.[11] values for the absolute proton solvation enthalpy (−274.9 kcal/mol) and Gibbs free energy (−264.0 kcal/mol). Both of the absolute proton hydration entropy values obtained from the cluster pair correlation method using the two different ion data sets (−39.8 and −36.6 cal/(mol·K)) are significantly more negative than the value measured directly in bulk solution by Conway and Wilkinson (−30.7 ± 0.7 cal/(mol·K)).[110] This latter value, obtained from bulk measurements, is referenced to the proton in the bulk of aqueous solution and should not include an entropic contribution from the surface potential of water.[112] However, because the temperature dependence of the surface potential of water is negative (∼−1.0 ± 0.5 mV/K),[34] including the entropic contribution from the surface potential of the interfacial water increases the absolute proton solvation entropy value to a less negative value, and would lead to even more severe disagreement between the entropy value obtained from the cluster pair correlation method and the directly measured value.

Conclusions

The cluster pair correlation method originally developed by Coe, Tuttle, and co-workers[25] for obtaining a value for the absolute proton hydration free energy from gaseous cluster data is clever and remarkably robust. We evaluated this method with a substantially larger experimental data set that includes 19 more ions (a total of 1129 more data points) than that used previously[10] and found that the resulting absolute proton hydration free energy is −259.3 kcal/mol, a value that is ∼4.5 kcal/mol less negative than previously reported values obtained using this method with smaller data sets,[10,25] indicating that the uncertainty in this method may be larger than previously appreciated. We found a new method of plotting and analyzing these data which results in a 5.7 kcal/mol more negative value than the conventional method[10,25] when using the larger data set. This improved cluster pair correlation method has the advantage of better precision and effects of cluster size can be more readily evaluated than the original method[10,25] or the cluster pair approximation method.[11]

Using this new method, solvation energies for ions with extreme pK_as were found to be unreliable and these ions, many of which were included in a previous data set used to obtain a value for the absolute proton hydration free energy,[10] were removed from the larger data set. With the new data set and the improved method, the "best" value for the standard absolute proton hydration free energy is −263.4 kcal/mol, which is the average value for the three largest clusters with 4−6 water molecules. The key assumption that is inherent in this method is that sequential solvation energies for ideal ion pairs of opposite polarity that are the same for small clusters will also be the same for larger clusters.

Although the precision of this improved cluster pair correlation method is excellent, the dependence of the absolute proton hydration free energy values on data set size indicates that the overall uncertainty of this method is much higher. There is also a slight trend in these values as a function of cluster size, and a much more significant trend is obtained for the enthalpy values. The absolute proton hydration enthalpy values decrease from −273.1 kcal/mol for clusters with one water molecule to −275.3 for clusters with six water molecules. The trend in enthalpy values with increasing cluster size, along with an anomalously high absolute proton hydration entropy obtained with this method, suggests that these enthalpy values obtained with the cluster pair correlation method may not have converged using data for clusters with up to 6 water molecules. Because of the discrepancy between the entropy value obtained from the cluster pair correlation method and the directly measured value, and the dependence of the absolute proton hydration enthalpy and, to a lesser extent, the absolute proton free energy value, on cluster size, as well as the dependence of these values on data set size and ion identity, it is difficult to confidently determine the overall uncertainty in the values obtained for the absolute proton solvation energy and enthalpy using the cluster pair correlation method. Although limited at this time, inclusion of more extensive experimental data for larger clusters, as it becomes available, would provide a better indication of the overall accuracy of this method.

Acknowledgment. Acknowledgment is made to the donors of the American Chemical Society Petroleum Research Fund (47916-AC6) for support of this research. The authors thank the National Science Foundation (CHE-0718790) for generous financial support.

Supporting Information Available: Tables of relative ion hydration free energies and enthalpies, and sequential ion hydration free energies and enthalpies used to evaluate the original and improved cluster pair correlation method. Description of how the ordinate value for the intersection points between two lines and the corresponding propagated uncertainty values are obtained. This material is available free of charge via the Internet at http://pubs.acs.org.

References and Notes

(1) Coe, J. V. *Int. Rev. Phys. Chem.* **2001**, *20*, 33.
(2) Cramer, C. J.; Truhlar, D. G. *Chem. Rev.* **1999**, *99*, 2161.
(3) Tomasi, J.; Persico, M. *Chem. Rev.* **1994**, *94*, 2027.
(4) Born, M. *Z. Phys.* **1920**, *1*, 45.
(5) Kelly, C. P.; Cramer, C. J.; Truhlar, D. G. *J. Chem. Theory Comput.* **2005**, *1*, 1133.
(6) Marenvich, A. V.; Olson, R. M.; Kelly, C. P.; Cramer, C. J.; Truhlar, D. G. *J. Chem. Theory Comput.* **2007**, *3*, 2011.
(7) Pliego, J. R., Jr.; Riveros, J. M. *Phys. Chem. Chem. Phys.* **2002**, *4*, 1622.
(8) Winget, P.; Cramer, C. J.; Truhlar, D. G. *Theor. Chem. Acc.* **2004**, *112*, 217.

(9) Torres, R. A.; Lovell, T.; Noodleman, L.; Case, D. A. *J. Am. Chem. Soc.* **2003**, *125*, 1923.
(10) Kelly, C. P.; Cramer, C. J.; Truhlar, D. G. *J. Phys. Chem. B* **2006**, *110*, 16081.
(11) Tissandier, M. D.; Cowen, K. A.; Feng, W. Y.; Gundlach, E.; Cohen, M. H.; Earhart, A. D.; Coe, J. V.; Tuttle, T. R., Jr. *J. Phys. Chem. A* **1998**, *102*, 7787.
(12) Marcus, Y. *Ion Properties*; Marcel Dekker: New York, 1997.
(13) Fawcett, W. R. *J. Phys. Chem. B* **1999**, *103*, 11181.
(14) Farrell, J. R.; McTigue, P. *J. Electroanal. Chem.* **1982**, *139*, 37.
(15) Trasatti, S. *Pure App. Chem.* **1986**, *58*, 955.
(16) Parsons, R. In *Standard Potentials in Aqueous Solution*; Bard, A. J., Parsons, R., Jordan, J., Eds.; Marcel Dekker: New York, 1985; p 13.
(17) Fawcett, W. R. *Langmuir* **2008**, *24*, 9868.
(18) Randles, J. E. B. *Trans. Faraday Soc.* **1956**, *52*, 1573.
(19) Tawa, G. J.; Topol, I. A.; Burt, S. K.; Caldwell, R. A.; Rashin, A. A. *J. Chem. Phys.* **1998**, *109*, 4852.
(20) Zhan, C.-G.; Dixon, D. A. *J. Phys. Chem. A* **2001**, *2001*, 11534.
(21) Bryantsev, V. S.; Diallo, M. S.; Goddard, W. A., III. *J. Phys. Chem. B* **2008**, *112*, 9709.
(22) Mejias, J. A.; Lago, S. *J. Chem. Phys.* **2000**, *113*, 7306.
(23) Klots, C. E. *J. Phys. Chem.* **1981**, *85*, 3585.
(24) Coe, J. V. *Chem. Phys. Lett.* **1994**, *229*, 161.
(25) Tuttle, T. R., Jr.; Malaxos, S.; Coe, J. V. *J. Phys. Chem. A* **2002**, *106*, 925.
(26) Kelly, C. P.; Cramer, C. J.; Truhlar, D. G. *J. Phys. Chem. B* **2007**, *111*, 408.
(27) Bartels, D. M.; Takahashi, K.; Cline, J. A.; Marin, T. W.; Jonah, C. D. *J. Phys. Chem. A* **2005**, *109*, 1299.
(28) Donald, W. A.; Leib, R. D.; Demireva, M.; O'Brien, J. T.; Prell, J. S.; Williams, E. R. *J. Am. Chem. Soc.* **2009**, *131*, 13328.
(29) Donald, W. A.; Leib, R. D.; O'Brien, J. T.; Bush, M. F.; Williams, E. R. *J. Am. Chem. Soc.* **2008**, *130*, 3371.
(30) Donald, W. A.; Leib, R. D.; O'Brien, J. T.; Williams, E. R. *Chem.—Eur. J.* **2009**, *15*, 5926.
(31) Randles, J. E. B. *Phys. Chem. Liq.* **1977**, *7*, 107.
(32) Kathmann, S. M.; Kuo, I.-F. W.; Mundy, C. J. *J. Am. Chem. Soc.* **2008**, *130*, 16556.
(33) Sokhan, V. P.; Tildesley, D. J. *Mol. Phys.* **1997**, *92*, 625.
(34) Farrell, J. R.; McTigue, P. *J. Electroanal. Chem.* **1984**, *163*, 129.
(35) Isse, A. A.; Gennaro, A. *J. Phys. Chem. B* **2010**, *114*, 7894.
(36) Donald, W. A.; Demireva, M.; Leib, R. D.; Aiken, M. J.; Williams, E. R. *J. Am. Chem. Soc.* **2010**, *132*, 4633.
(37) Donald, W. A.; Leib, R. D.; Demireva, M.; Negru, B.; Neumark, D. M.; Williams, E. R. *J. Am. Chem. Soc.* **2010**, *132*, 6904.
(38) Donald, W. A.; Leib, R. D.; O'Brien, J. T.; Holm, A. I. S.; Williams, E. R. *Proc. Natl. Acad. Sci. U.S.A.* **2008**, *105*, 18102.
(39) Donald, W. A.; Williams, E. R. *J. Am. Soc. Mass Spectrom.* **2010**, *21*, 615.
(40) Leib, R. D.; Donald, W. A.; Bush, M. F.; O'Brien, J. T.; Williams, E. R. *J. Am. Chem. Soc.* **2007**, *129*, 4894.
(41) Leib, R. D.; Donald, W. A.; Bush, M. F.; O'Brien, J. T.; Williams, E. R. *J. Am. Soc. Mass Spectrom.* **2007**, *18*, 1217.
(42) Leib, R. D.; Donald, W. A.; O'Brien, J. T.; Bush, M. F.; Williams, E. R. *J. Am. Chem. Soc.* **2007**, *129*, 7716.
(43) Holm, A. I. S.; Donald, W. A.; Hvelplund, P.; Larsen, M. K.; Nielsen, S. B.; Williams, E. R. *J. Phys. Chem. A* **2008**, *112*, 10721.
(44) Kebarle, P. In *Modern Aspects of Electrochemistry*; Conway, B. E., Bockris, J. O. M., Eds.; Plenum Press: New York, 1974; Vol. 9, p 29.
(45) Desnoyers, J. E.; Jolicoeur, C. In *Modern Aspects of Electrochemistry*; Bockris, J. O. M., Conway, B. E., Eds.; Plenum Press: New York, 1969; Vol. 5, p 20.
(46) Camaioni, D. M.; Schwerdtfeger, C. A. *J. Phys. Chem. A* **2005**, *109*, 10795.
(47) Rodgers, M. T.; Armentrout, P. B. *J. Phys. Chem. A* **1997**, *101*, 1238.
(48) Dzidic, I.; Kebarle, P. *J. Phys. Chem.* **1970**, *74*, 1466.
(49) McMahon, T. B.; Ohanessian, G. *Chem.—Eur. J.* **2000**, *6*, 2931.
(50) Burdett, N. A.; Hayhurst, A. N. *J. Chem. Soc., Faraday Trans. I* **1982**, *78*, 2997.
(51) Tang, I. N.; Castleman, A. W. *J. Chem. Phys.* **1972**, *57*, 3638.
(52) Tang, I. N.; Lian, M. S.; Castleman, A. W. *J. Chem. Phys.* **1976**, *65*, 4022.
(53) Blades, A. T.; Ho, Y. H.; Kebarle, P. *J. Am. Chem. Soc.* **1996**, *118*, 196.
(54) Blades, A. T.; Jayaweera, P.; Ikonomou, M. G.; Kebarle, P. *J. Chem. Phys.* **1990**, *92*, 5900.
(55) Blades, A. T.; Klassen, J. S.; Kebarle, P. *J. Am. Chem. Soc.* **1995**, *117*, 10563.
(56) Blades, A. T.; Klassen, J. S.; Kebarle, P. *J. Am. Chem. Soc.* **1996**, *118*, 12437.
(57) Castleman, A. W.; Holland, P. M.; Lindsay, D. M.; Peterson, K. I. *J. Am. Chem. Soc.* **1978**, *100*, 6039.
(58) Searles, S. K.; Kebarle, P. *Can. J. Chem.* **1969**, *47*, 2619.
(59) Davidson, W. R.; Kebarle, P. *J. Am. Chem. Soc.* **1976**, *98*, 6125.
(60) Davidson, W. R.; Sunner, J.; Kebarle, P. *J. Am. Chem. Soc.* **1979**, *101*, 1675.
(61) Banic, C. M.; Iribarne, J. V. *J. Chem. Phys.* **1985**, *83*, 6432.
(62) Holland, P. M.; Castleman, A. W. *J. Chem. Phys.* **1982**, *76*, 4195.
(63) Meotner, M. *J. Am. Chem. Soc.* **1984**, *106*, 1265.
(64) Meotner, M. *J. Am. Chem. Soc.* **1984**, *106*, 278.
(65) Meotner, M. *J. Am. Chem. Soc.* **1986**, *108*, 6189.
(66) Meotner, M. *J. Am. Chem. Soc.* **1988**, *110*, 3854.
(67) Meotner, M. *J. Am. Chem. Soc.* **1988**, *110*, 3858.
(68) Meotner, M.; Field, F. H. *J. Am. Chem. Soc.* **1977**, *99*, 998.
(69) Meotner, M.; Sieck, L. W. *J. Am. Chem. Soc.* **1983**, *105*, 2956.
(70) Meotner, M.; Sieck, L. W. *J. Phys. Chem.* **1985**, *89*, 5222.
(71) Meotner, M.; Sieck, L. W. *J. Am. Chem. Soc.* **1986**, *108*, 7525.
(72) Meotner, M.; Sieck, L. W. *J. Phys. Chem.* **1986**, *90*, 6687.
(73) Meotner, M.; Speller, C. V. *J. Phys. Chem.* **1986**, *90*, 6616.
(74) Cunningham, A. J.; Payzant, J. D.; Kebarle, P. *J. Am. Chem. Soc.* **1972**, *94*, 7627.
(75) Hiraoka, K.; Grimsrud, E. P.; Kebarle, P. *J. Am. Chem. Soc.* **1974**, *96*, 3359.
(76) Hiraoka, K.; Mizuse, S.; Yamabe, S. *J. Phys. Chem.* **1988**, *92*, 3943.
(77) Hiraoka, K.; Takimoto, H.; Morise, K. *J. Am. Chem. Soc.* **1986**, *108*, 5683.
(78) Hiraoka, K.; Takimoto, H.; Yamabe, S. *J. Am. Chem. Soc.* **1987**, *109*, 7346.
(79) Lau, Y. K.; Ikuta, S.; Kebarle, P. *J. Am. Chem. Soc.* **1982**, *104*, 1462.
(80) Lau, Y. K.; Kebarle, P. *Can. J. Chem.* **1981**, *59*, 151.
(81) Lau, Y. K.; Nishizawa, K.; Tse, A.; Brown, R. S.; Kebarle, P. *J. Am. Chem. Soc.* **1981**, *103*, 6291.
(82) Kebarle, P. *Annu. Rev. Phys. Chem.* **1977**, *28*, 445.
(83) Payzant, J. D.; Cunningham, A. J.; Kebarle, P. *Can. J. Chem.—Rev. Can. Chim.* **1973**, *51*, 3242.
(84) Elshall, M. S.; Daly, G. M.; Gao, J. L.; Meotner, M.; Sieck, L. W. *J. Phys. Chem.* **1992**, *96*, 507.
(85) Nicol, G.; Sunner, J.; Kebarle, P. *Int. J. Mass Spectrom. Ion Process.* **1988**, *84*, 135.
(86) Speller, C. V.; Meotner, M. *J. Phys. Chem.* **1985**, *89*, 5217.
(87) Weis, P.; Kemper, P. R.; Bowers, M. T.; Xantheas, S. S. *J. Am. Chem. Soc.* **1999**, *121*, 3531.
(88) Payzant, J. D.; Yamdagni, R.; Kebarle, P. *Can. J. Chem.* **1971**, *49*, 3308.
(89) Arshadi, M.; Kebarle, P. *J. Phys. Chem.* **1970**, *74*, 1483.
(90) Arshadi, M.; Yamdagni, R.; Kebarle, P. *J. Phys. Chem.* **1970**, *74*, 1475.
(91) Keesee, R. G.; Castleman, A. W. *Chem. Phys. Lett.* **1980**, *74*, 139.
(92) Paul, G. J. C.; Kebarle, P. *J. Phys. Chem.* **1990**, *94*, 5184.
(93) Kebarle, P.; Arshadi, M.; Scarboro, J. *J. Chem. Phys.* **1968**, *49*, 817.
(94) Larson, J. W.; Szulejko, J. E.; McMahon, T. B. *J. Am. Chem. Soc.* **1988**, *110*, 7604.
(95) Sieck, L. W.; Meotner, M. *J. Phys. Chem.* **1989**, *93*, 1586.
(96) Keesee, R. G.; Lee, N.; Castleman, A. W. *J. Am. Chem. Soc.* **1979**, *101*, 2599.
(97) Lee, N.; Keesee, R. G.; Castleman, A. W. *J. Chem. Phys.* **1980**, *72*, 1089.
(98) Sieck, L. W. *J. Phys. Chem.* **1985**, *89*, 5552.
(99) Rodgers, M. T.; Armentrout, P. B. *Mass Spectrom. Rev.* **2000**, *19*, 215.
(100) Magnera, T. F.; David, D. E.; Stulik, D.; Orth, R. G.; Jonkman, H. T.; Michl, J. *J. Am. Chem. Soc.* **1989**, *111*, 5036.
(101) The values for each cluster size are still dependent upon the values for the smaller cluster sizes because the sum of the sequential binding energies depend on the values for each of the smaller clusters.
(102) Stewart, R. *The Proton: Applications to Organic Chemistry*; Academic Press, Inc.: Orlando, FL, 1985.
(103) Isaacs, N. *Physical Organic Chemistry*, 2nd ed.; John Wiley and Sons, Inc.: New York, 1995.
(104) Lowry, T. H.; Richardson, K. S. *Mechanism and Theory in Organic Chemistry*, 3rd ed.; Harper International Edition; Harper & Row: New York, 1987.
(105) Solomons, G.; Fryhle, C. *Organic Chemistry*, 7th ed.; John Wiley and Sons Inc.: New York, 2002.
(106) Kresge, A. J.; Pruszynski, P.; Stang, P. J.; Williamson, B. L. *J. Org. Chem.* **1991**, *56*, 4808.
(107) Arnett, E. M. *Prog. Phys. Org. Chem.* **1963**, *1*, 223.
(108) Deno, N. C.; Gaugler, R. W.; Wisotsky, M. J. *J. Org. Chem.* **1966**, *31*, 1967.
(109) Lemaire, H.; Lucas, H. J. *J. Am. Chem. Soc.* **1951**, *73*, 5198.

(110) Conway, B. E.; Wilkinson, D. P. *Electrochim. Acta* **1993**, *38*, 997.

(111) de Bethune, A. J.; Licht, T. S.; Swendeman, N. *J. Electrochem. Soc.* **1959**, *106*, 616.

(112) Conway, B. E.; Salomon, M. In *Chemical Physics of Ionic Solutions*; Conway, B. E., Barradas, R. G., Eds.; Wiley: New York, 1966.

(113) Using a value of −108.9 cal/mol·K for the standard entropy of the proton in the gas phase obtained from: Chase, M. W., Jr. *NIST-JANAF Thermochemical Tables, Fourth ed., Part II, Cr-Zr*; American Institutes of Physics: Woodbury, NY, 1998.

JP1068945